

Molecular Physics

An International Journal at the Interface Between Chemistry and Physics

ISSN: (Print) (Online) Journal homepage: <https://www.tandfonline.com/loi/tmph20>

Atmospheric chemistry of diazomethane – an experimental and theoretical study

Simen Gjelseth Antonsen , Arne Joakim C. Bunkan , Tomas Mikoviny , Claus J. Nielsen , Yngve Stenstrøm , Armin Wisthaler & Erika Zardin

To cite this article: Simen Gjelseth Antonsen , Arne Joakim C. Bunkan , Tomas Mikoviny , Claus J. Nielsen , Yngve Stenstrøm , Armin Wisthaler & Erika Zardin (2020) Atmospheric chemistry of diazomethane – an experimental and theoretical study, Molecular Physics, 118:15, e1718227, DOI: [10.1080/00268976.2020.1718227](https://doi.org/10.1080/00268976.2020.1718227)

To link to this article: <https://doi.org/10.1080/00268976.2020.1718227>



© 2020 The Author(s). Published by Informa UK Limited, trading as Taylor & Francis Group



Published online: 30 Jan 2020.



Submit your article to this journal [↗](#)



Article views: 427



View related articles [↗](#)





View Crossmark data [↗](#)



Citing articles: 1 View citing articles [↗](#)

Atmospheric chemistry of diazomethane – an experimental and theoretical study

Simen Gjølseth Antonsen^a, Arne Joakim C. Bunkan^b, Tomas Mikoviny^b, Claus J. Nielsen ^b, Yngve Stenstrøm^a, Armin Wisthaler ^b and Erika Zardin^b

^aDepartment of Chemistry, Biotechnology and Food Science, Aas, Norway; ^bDepartment of Chemistry, University of Oslo, Oslo, Norway

ABSTRACT

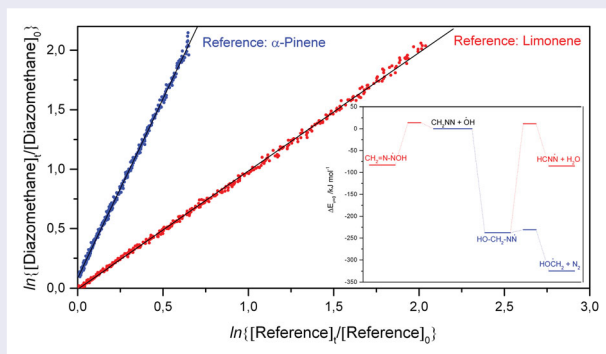
The kinetics of the O₃, OH and NO₃ radical reactions with diazomethane were studied in smog chamber experiments employing long-path FTIR and PTR-ToF-MS detection. The rate coefficients were determined to be $k_{\text{CH}_2\text{NN}+\text{O}_3} = (3.2 \pm 0.4) \times 10^{-17}$ and $k_{\text{CH}_2\text{NN}+\text{OH}} = (1.68 \pm 0.12) \times 10^{-10}$ cm³ molecule⁻¹ s⁻¹ at 295 ± 3 K and 1013 ± 30 hPa, whereas the CH₂NN + NO₃ reaction was too fast to be determined in the static smog chamber experiments. Formaldehyde was the sole product observed in all the reactions. The experimental results are supported by CCSD(T*)-F12a/aug-cc-pVTZ//M062X/aug-cc-pVTZ calculations showing the reactions to proceed exclusively via addition to the carbon atom. The atmospheric fate of diazomethane is discussed.

ARTICLE HISTORY

Received 14 November 2019
Accepted 5 January 2020

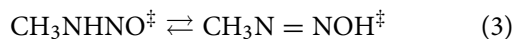
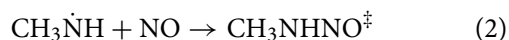
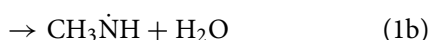
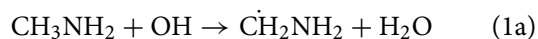
KEYWORDS

Atmospheric chemistry; reaction mechanism; amine photo-oxidation; quantum chemistry

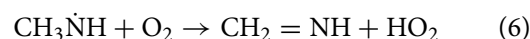
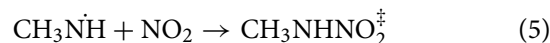


Introduction

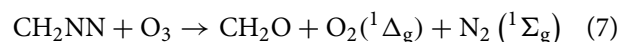
Diazomethane, CH₂NN, was recently predicted to result in a rearrangement of *N*-nitroso methylamine, which is formed with around 200 kJ mol⁻¹ internal energy in the atmospheric photo-oxidation of methylamine [1]:




Under atmospheric conditions the CH₃ $\dot{\text{N}}\text{H}$ radicals also reacts with NO₂ and O₂, and it should be noted that the major atmospheric sink for CH₃ $\dot{\text{N}}\text{H}$ by far is reaction with O₂ [2,3]:



There is little information in the literature on the atmospheric fate of diazomethane. The compound was reported to be formed in methylhydrazine ozonolysis experiments and found to react relatively fast in the presence of ppm-levels of O₃ to give formaldehyde [4]. No rate coefficient for the O₃ reaction was presented.



CONTACT Claus J. Nielsen  claus.nielsen@kjemi.uio.no  Department of Chemistry, University of Oslo, P.O.Box. 1033, 0315 Oslo, Norway

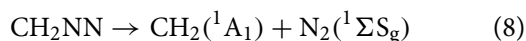
 Supplemental data for this article can be accessed here. <https://doi.org/10.1080/00268976.2020.1718227>

© 2020 The Author(s). Published by Informa UK Limited, trading as Taylor & Francis Group

This is an Open Access article distributed under the terms of the Creative Commons Attribution-NonCommercial-NoDerivatives License (<http://creativecommons.org/licenses/by-nc-nd/4.0/>), which permits non-commercial re-use, distribution, and reproduction in any medium, provided the original work is properly cited, and is not altered, transformed, or built upon in any way.

CH₂NN has strong absorption bands below 300 nm but only a very weak, forbidden $\pi \rightarrow \pi^*$ transition around 400 nm with a maximum molar attenuation coefficient of $\sim 3 \text{ M}^{-1} \text{ cm}^{-1}$ (absorption cross section $\sim 10^{-21} \text{ cm}^2 \text{ molecule}^{-1}$) [5–7]; there is no information available on the quantum yield to photo-dissociation. Assuming a quantum yield of 1 over the entire 300–500 nm range of the absorption band and an average Actinic flux of $14^{14} \text{ quanta cm}^{-2} \text{ s}^{-1} (\text{nm})^{-1}$ in this region [8], the estimated lifetime with respect to photolysis will be around 1 d. Tropospheric photolysis may, nonetheless, constitute an important atmospheric sink for diazomethane.

Diazomethane is reported to dissociate in a highly endothermic process; $E_a \sim 280 \text{ kJ mol}^{-1}$ [9]:



The high-pressure rate coefficient was recently calculated to be $\sim 10^{-10} \text{ s}^{-1}$ at 295 K [10], and the thermal dissociation is obviously far too slow to be of importance under atmospheric conditions.

Finally, diazomethane is stated to undergo rapid hydrolysis to give methanol in acidic solution [11], making removal from the atmosphere by aqueous particles of potential significance.

In the present study we address the atmospheric fate of diazomethane and report results from smog chamber studies of the diazomethane reactions with O₃, OH and NO₃ radicals supported by quantum chemistry calculations of the potential energy surfaces of the reactions.

Experimental and computational methods

Experimental methods

The experiments were performed in synthetic air (PRAX-AIR 5.0) at $295 \pm 2 \text{ K}$ and $1013 \pm 50 \text{ mbar}$ in a 250 L electropolished stainless-steel reactor. The kinetic studies of the CH₂NN + O₃ reaction were carried out monitoring the absolute mixing ratio of O₃ and the relative mixing ratio of CH₂NN. The rate coefficient was extracted from the experiments by numerical modelling of the observed CH₂NN decay as a function of time.

$$\frac{d[\text{CH}_2\text{NN}]}{dt} = -k \cdot [\text{CH}_2\text{NN}] \cdot [\text{O}_3]; [\text{O}_3] = f(t)$$

where the function $f(t)$ was approximated by an exponential decay curve.

The kinetic studies of the CH₂NN reactions with OH and NO₃ radicals were carried out by the relative rate method in a static gas mixture, in which the removals of the reacting species are measured simultaneously as a function of reaction time. Assuming that the compounds

under study react solely with the same radical species and that none of the compounds are reformed in any side reactions, the relative rate coefficient, k_{rel} , is given according to the following expression:

$$\ln\left\{\frac{[\text{CH}_2\text{NN}]_0}{[\text{CH}_2\text{NN}]_t}\right\} = k_{rel} \cdot \ln\left\{\frac{[\text{Ref}]_0}{[\text{Ref}]_t}\right\};$$

$$k_{rel} = k_{\text{CH}_2\text{NN}}/k_{\text{Ref}}$$

where $[\text{CH}_2\text{NN}]_0$, $[\text{CH}_2\text{NN}]_t$, $[\text{Ref}]_0$ and $[\text{Ref}]_t$ are the concentrations of diazomethane and the reference compound at start and at the time t , respectively, and $k_{\text{CH}_2\text{NN}}$ and k_{Ref} are the corresponding rate coefficients for their reactions with either OH or NO₃. A plot of $\ln\{[\text{CH}_2\text{NN}]_0/[\text{CH}_2\text{NN}]_t\}$ vs. $\ln\{[\text{Ref}]_0/[\text{Ref}]_t\}$ will thus give the relative reaction rate coefficient $k_{rel} = k_{\text{CH}_2\text{NN}}/k_{\text{Ref}}$ as the slope.

FT-IR

The Oslo Smog Chamber is equipped with a White multi-reflection mirror system adjusted to give an optical path length of 120 m and interfaced to a Bruker IFS-66v/S FTIR spectrometer for in situ analysis. FTIR spectra were obtained by co-adding 32 interferograms with a resolution of 0.5 cm^{-1} . Boxcar apodisation was used in the Fourier transformation.

Proton-transfer-reaction time-of-flight mass spectrometer (PTR-TOF-MS)

A commercial PTR-TOF 8000 instrument (Ionicon Analytik GmbH, Innsbruck, Austria) was used for on-line organic trace gas measurements [12]. The instrument was operated at 100 Td ($1 \text{ Td} = 10^{-17} \text{ V cm}^{-2} \text{ molecule}^{-1}$) in a 1–4 s integration mode; the drift tube was kept at a temperature of 50 °C and a pressure of 2.8 mbar. The analyzer was interfaced to the Oslo chamber via a 150 cm long stainless steel/PEEK tubing kept at room temperature. The inlet flow was set to 300 sccm.

Instrumental data analysis. The spectra collected by the PTR-ToF-MS were analysed with PTR-MS Viewer ver. 3.2.14 (Ionicon Analytik GmbH, Innsbruck, Austria). The mass scale of the spectra was consistently aligned with a three-points calibration using a permanent internal reference substance (1,2-diiodobenzene, CAS Number 615-42-9). Multiple peaks were manually fitted in the software to maximise the accuracy of the resulting signals in counts per second (cps).

Ozone monitor

A model 49C O₃ Analyzer from Thermo Environmental Instruments Inc. was used to monitor the ozone levels in the smog chamber.

Chemicals

Methylamine hydrochloride (Sigma-Aldrich, $\geq 98\%$), urea (Sigma-Aldrich, ReagentPlus[®], $\geq 99\%$), sodium nitrite (Sigma-Aldrich, ReagentPlus[®], $\geq 99\%$), potassium hydroxide (Sigma-Aldrich, ACS reagent, $\geq 85\%$ pellets), isoprene (Sigma-Aldrich, 99%), (R)-(+)-limonene (Sigma-Aldrich, 97%). Ozone was produced from oxygen (99.995%; AGA) using an MK II Ozone generator from BOC, which has a conversion efficiency of approximately 5%. N_2O_5 was produced by mixing gas streams of NO_2 and O_3 and trapping the products at -79°C . 1,1,1,3,3,3-Hexadeutero-2-propyl nitrite (IPN-d6) was synthesised from 1,1,1,3,3,3-hexadeutero-2-propanol, 35% hydrochloric acid and sodium nitrite, and purified by repeated washing with ice water.

Diazomethane was prepared in mmol scale by adding excess 50% aqueous KOH to solid nitrosomethylurea. Nitrosomethylurea was synthesised from methylamine and urea as described by Arndt, [13] with some modifications. Diazomethane is reported to be explosive and all safety measures should be taken accordingly [14]. Methylamine hydrochloride (5.0 g, 0.075 mol) was dissolved in water (50 mL). Urea (15 g, 0.25 mol) was added. The mixture was heated to reflux for 3 h, then cooled to room temperature. Sodium nitrite (5.5 g, 0.075 mol) was added and allowed to dissolve at room temperature. The mixture was cooled to 0°C and poured into a beaker containing ice (30 g) and sulphuric acid (5.0 g, 0.050 mol). Nitrosomethylurea precipitates as fluffy, slightly yellow crystals, which is filtered with suction. The precipitate is washed with cold water (10 mL), and the solid is dried in desiccator over night to give nitrosomethylurea (5.2 g, 0.050 mol).

Quantum chemical methods

Stationary points on the potential energy surface for the reactions of O_3 , OH and NO_3 with diazomethane were characterised in M062X [15] calculations employing the aug-cc-pVTZ [16,17] basis sets. The energies of the stationary points were then improved with explicitly correlated coupled cluster singles and doubles calculations with perturbative triples scaled, denoted CCSD(T*)-F12a [18,19]. Saddle points on the potential energy surfaces (PES) of reactions were located by scanning the bonds formed/broken and subsequently validated in intrinsic reaction coordinate (IRC) calculations [20].

Reaction enthalpies and proton affinities were calculated using the G4 model chemistry [21]. The coupled cluster calculations were performed in Molpro 2012.1 [22], whereas the DFT and G4 calculations were performed in Gaussian 09 [23].

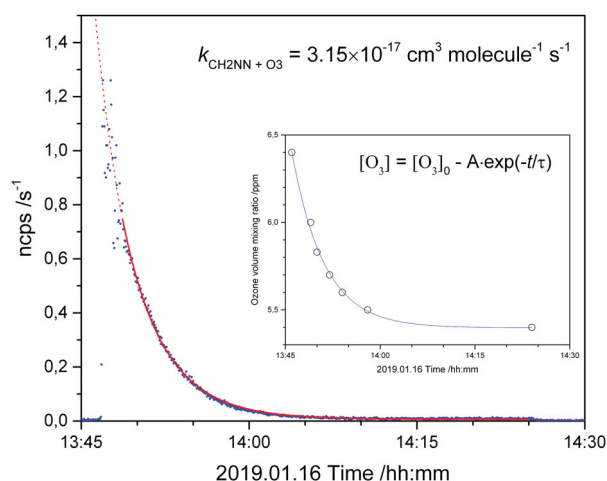


Figure 1. Normalised counts per second of the m/z 43.028 ion signal (CH_3N_2^+) as a function of time during a $\text{CH}_2\text{NN} + \text{O}_3$ experiment. Full red curve: modelled CH_2N_2 decay. Dotted red curve: extrapolated model results. Inserted plot shows the O_3 decay during the experiment.

Results and discussion

Diazomethane was synthesised in a small glass bulb and introduced directly to the smog chamber in a stream of clean air. Figure S1 shows that the IR spectrum obtained conforms with the literature [24–26]. Upon gas phase protonation in the PTR-ToF-MS ion source significant fragmentation takes place and correlated ion signals were observed by at m/z 15.024 (CH_3^+), 33.034 (CH_5O^+) and 43.030 (CH_3N_2^+). Absolute quantification of diazomethane in the chamber by PTR-ToF-MS and FTIR was not pursued.

The stability of diazomethane in the chamber clean air was investigated in separate experiments. Assuming the apparent sample loss to be of first order, a rate coefficient of $< 5 \times 10^{-5} \text{ s}^{-1}$ was obtained. This corresponds to a lifetime of $> 6\text{h}$ in the chamber, and the ‘natural’ chamber loss of diazomethane will therefore not impact the kinetic analyses, see below. The photo stability of diazomethane towards 305 nm radiation from the photolysis lamps in clean air was also examined; less than 1% of the compound was photolysed during a one-hour exposure.

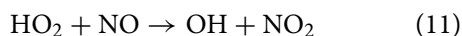
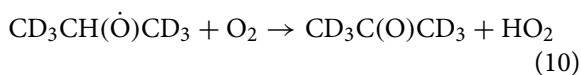
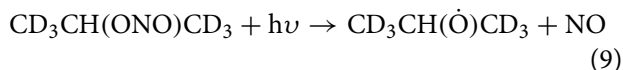
Kinetics of the $\text{CH}_2\text{NN} + \text{O}_3$ reaction

Six experiments with varying amounts of CH_2NN and O_3 were carried out. Diazomethane reacts relatively fast with O_3 , and the experimental conditions were never such that a pseudo first-order approximation could be employed in the analyses. Figure 1 shows the results from the first experiment whereas the other 5 experiments are documented in Figures S2–S6.

The rate coefficients derived in modelling the experimental data according to equation I vary between 2.95 and $3.4 \times 10^{-17} \text{ cm}^3 \text{ molecule}^{-1} \text{ s}^{-1}$ – (3.15, 2.95, 3.35, 3.25, 3.35 and $3.4 \times 10^{-17} \text{ cm}^3 \text{ molecule}^{-1} \text{ s}^{-1}$; all having an estimated 10% uncertainty). We endorse the average result (with 2σ error limit) as our best value for the rate coefficient: $k_{\text{CH}_2\text{NN}+\text{O}_3} = (3.2 \pm 0.4) \times 10^{-17} \text{ cm}^3 \text{ molecule}^{-1} \text{ s}^{-1}$ at 295 K and atmospheric pressure.

Kinetics of the $\text{CH}_2\text{NN} + \text{OH}$ reaction

The OH radicals were generated by photolysis of 2-propylnitrite-1,1,1,3,3,3- d_6 (IPN-d6) employing Philips TL 20W/12 fluorescence lamps ($\lambda_{\text{max}} \sim 305 \text{ nm}$) inserted in a quartz tube mounted into the reaction chamber. IPN-d6 was used to reduce potential interferences in the MS spectra. The mechanism for OH production from photolysis of IPN-d6 is as follows:



Separate experiments were carried out to investigate direct photolysis of diazomethane by the photolysis lamps. The maximum emission of the fluorescence lamps falls at the minimum absorption of diazomethane (absorption cross section $\sim 10^{-22} \text{ cm}^2 \text{ molecule}^{-1}$ from 250 to 315 nm) [5–7], and less than 1% loss of diazomethane loss due to direct photolysis occurred during the time of a typical RR experiment ($\sim 30 \text{ min}$). The impact of direct photolysis can therefore be neglected in the analyses of the kinetic experiments.

Relative rate experiments were carried out employing limonene ($k_{\text{OH}+\text{limonene}} = 1.68 \times 10^{-10} \text{ cm}^3 \text{ molecule}^{-1} \text{ s}^{-1}$; $\Delta \log k = \pm 0.05$ at 295 K [27]) and α -pinene ($k_{\text{OH}+\alpha\text{-pinene}} = 5.38 \times 10^{-11} \text{ cm}^3 \text{ molecule}^{-1} \text{ s}^{-1}$; $\Delta \log k = \pm 0.08$ at 295 K [27]) as reference compounds; Figure 2 illustrates the results. Two experiments were carried out for each reference compound giving averages $k_{\text{Diazomethane}+\text{OH}}/k_{\text{Limonene}+\text{OH}} = 1.026 \pm 0.045$ and $k_{\text{Diazomethane}+\text{OH}}/k_{\alpha\text{-pinene}+\text{OH}} = 3.041 \pm 0.041$ from which an absolute rate coefficient with 2σ error limit $k_{\text{Diazomethane}+\text{OH}} = (1.68 \pm 0.12) \times 10^{-10} \text{ cm}^3 \text{ molecule}^{-1} \text{ s}^{-1}$ at 295 K is extracted.

Kinetics of the $\text{CH}_2\text{NN} + \text{NO}_3$ reaction

The NO_3 radicals were generated *in situ* by thermal dissociation of N_2O_5 ($\text{N}_2\text{O}_5 \rightleftharpoons \text{NO}_2 + \text{NO}_3$). The NO_3 reaction with CH_2NN was so fast that all CH_2NN had

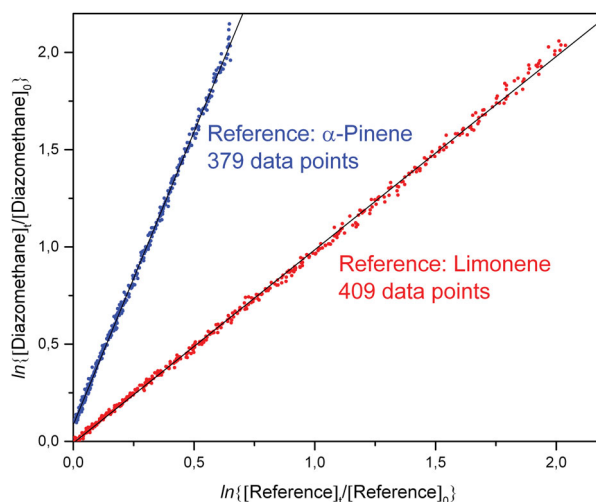


Figure 2. (A) Decays of diazomethane, limonene and α -pinene in the presence of OH radicals in 1 of the 2 experiments carried out. The data have been plotted as $\ln\{[\text{Diazomethane}]_0/[\text{Diazomethane}]_t\}$ vs. respectively $\ln\{[\text{Limonene}]_0/[\text{Limonene}]_t\}$ or $\ln\{[\alpha\text{-Pinene}]_0/[\alpha\text{-Pinene}]_t\}$. Analysis of the data points shown give relative rate coefficients $k_{\text{Diazomethane}+\text{OH}}/k_{\text{Limonene}+\text{OH}} = 0.9941 \pm 0.0017$ and $k_{\text{Diazomethane}+\text{OH}}/k_{\alpha\text{-Pinene}+\text{OH}} = 3.012 \pm 0.006$ (1σ). The α -pinene data have been shifted for the sake of clarity.

reacted during the time a stream of NO_2 and N_2O_5 containing air was introduced to the smog chamber ($< 1 \text{ min}$). It was not possible to distinguish between the NO_3 reactivities of CH_2NN and the reference compound (1,3-cyclohexadiene, $k_{\text{C}_6\text{H}_8+\text{NO}_3} = 1.2 \times 10^{-11} \text{ cm}^3 \text{ molecule}^{-1} \text{ s}^{-1}$ [28]) indicating similar rate coefficients for the NO_3 reactions with the two compounds. The alternative method to generate NO_3 radicals in the smog chamber from NO_2 and O_3 could not be used because CH_2NN and the relevant reference compounds also react with O_3 .

Quantum chemistry results

The bonding in diazomethane has previously been thoroughly characterised in CASPT2 and CASPT3 calculations showing that there is virtually no total charge transfer between the $-\text{CH}_2$ and $-\text{N}_2$ moieties, that the carbon and terminal nitrogen atoms have net negative charges, and that the CN bond consists of a single σ -bond, originating from the σ electrons of central nitrogen and a π -like bond due to the back-transfer of the carbon π electrons: [29]

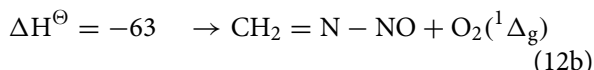
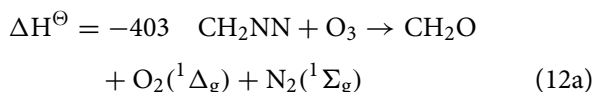


The electronic structures obtained in our MP2/aug-cc-pVTZ and M062X/aug-cc-pVTZ calculations of

CH₂NN comply with this depiction although the Mulliken charges obtained at the MP2 and M062X levels are significantly larger than the CASPT2 values [29]. Nonetheless, the MP2/M062X calculated dipole moments (1.47 / 1.53 D) and the structural parameters ($r_{\text{CH}} = 1.073 / 1.074$ Å, $r_{\text{CN}} = 1.310 / 1.292$ Å, $r_{\text{NN}} = 1.138 / 1.124$ Å and $\alpha_{\text{HCH}} = 126 / 125^\circ$) agree as well as can be expected with experiment ($\mu = 1.45$ D and (r_0 -structure) $r_{\text{CH}} = 1.08$ Å, $r_{\text{CN}} = 1.32$ Å, $r_{\text{NN}} = 1.12$ Å and $\alpha_{\text{HCH}} = 127^\circ$) [30].

CH₂NN + O₃

In accordance with the electronic structure outlined above for CH₂NN the CH₂NN + O₃ reaction proceeds either via addition to the carbon atom, leading to formaldehyde, or via addition to the terminal nitrogen atom, leading to *N*-nitroso methanimine (reaction enthalpies presented in kJ mol⁻¹ stem from G4 calculations [21]):

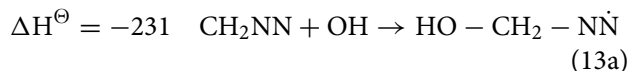


The N-addition reaction 12b is calculated with a barrier of more than 100 kJ mol⁻¹ and is obviously of no importance under atmospheric conditions; the extremely exothermic C-addition reaction 12a is calculated with a barrier of only 15.6 kJ mol⁻¹ ($\Delta G^\ddagger = 60.4$ kJ mol⁻¹), from which a rate coefficient of 6.4×10^{-18} cm³ molecule⁻¹ s⁻¹ at 295 K is predicted from Conventional Transition State Theory. We are aware that ozone is a challenging molecule to describe in simple quantum chemistry calculations, see, e.g. Reference [31]. This is also evidenced in our M06-2X/aug-cc-pVTZ results having OO distances that are 0.04 Å too short compared to experiment [32], and with the two OO stretching vibrations correspondingly calculated > 200 cm⁻¹ higher than observed [33]. Multireference methods are needed to improve the theoretical description not only of ozone itself, but also of the saddle point structures to reaction, for which the T₁ [34] and D₁ [35,36] diagnostic values for the CCSD calculation are uncomfortably large. In spite of this obvious fallacy, the theoretical results concord well with experiment; a lowering of the calculated barrier height by 4 kJ mol⁻¹ will result in a 5 times larger rate coefficient and a perfect agreement with experiment.

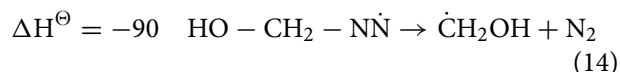
The T₁ and D₁ diagnostics values, energies, Cartesian Coordinates and vibration-rotation data for reactants and products in the CH₂NN + O₃ reaction are summarised in Table S1.

CH₂NN + OH

The OH radical reaction with CH₂NN may occur either as an addition to the carbon, an addition to the terminal nitrogen atom, or as a hydrogen abstraction:



The C-addition reaction 13a is found to proceed without any electronic barrier and to advance from the initially formed HO-CH₂-NN adduct via an almost negligible submerged barrier to the formaldehyde precursor CH₂OH:



The N-addition reaction 13b is found with a barrier of around 14 kJ mol⁻¹ ($\Delta G^\ddagger = 45.9$ kJ mol⁻¹, $k_{\text{CTST}} \sim 10^{-15}$ cm³ molecule⁻¹ s⁻¹ at 298 K). The abstraction reaction 13c is calculated with a barrier of around 11 kJ mol⁻¹ above the entrance energy of the reactants, and to proceed via the HO-CH₂-NN adduct on the entrance side and a H-bonded complex, HCNN•H₂O, on the exit side ($\Delta G^\ddagger = 41.7$ kJ mol⁻¹, $k_{\text{CTST}} \sim 10^{-11}$ cm³ molecule⁻¹ s⁻¹ at 298 K). The potential energy surface (PES) of reactions 13–14 is illustrated in Figure 3 (the underlying quantum chemistry data are collected in Table S2). It is obvious from the PES that the reaction will proceed entirely via the C-addition route with a rate close to the collision limit, $\sim 4.0 \times 10^{-10}$ cm³ molecule⁻¹ s⁻¹ at 295 K and 1 atm.

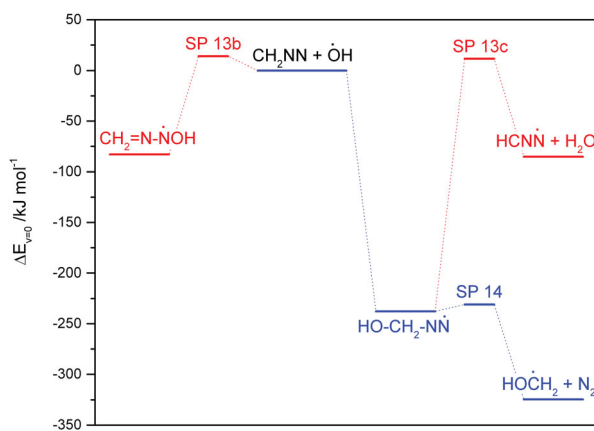


Figure 3. Stationary points on the potential energy surface of the CH₂NN + OH reaction. Results from CCSD(T*)-F12a/aug-cc-pVTZ//M06-2X/aug-cc-pVTZ calculations.

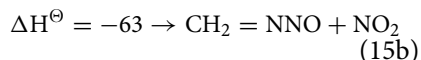
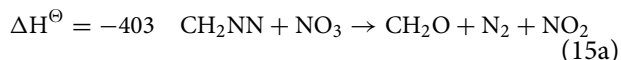
CH₂NN + NO₃

The NO₃ radical presents a computational challenge. Due to symmetry breaking it is not possible to calculate the electronic structure of the NO₃ radical correct using any standard size extensive UHF wave function based method that is also applicable to larger systems [37]. Many DFT methods show the same symmetry breaking, and this issue is all too often disregarded in theoretical studies of NO₃ radical reactions. The electronic ground state of the NO₃ radical has *D*_{3h} symmetry (\tilde{X}^2A_2') [38,39]. The M06-2X hybrid functional, however, predicts the *D*_{3h} structure as a saddle point and locates two minimum energy structures of *C*_{2v} symmetry having respectively 2 short and 1 long NO distance (2*s*1*l*), and 1 short and 2 long NO distances (1*s*2*l*). Table S3 summarises the results obtained for the *D*_{3h} and the two *C*_{2v} structures obtained in the M06-2X calculations.

The quantum chemistry model electronic energy of the NO₃ radical was obtained by combining the theoretical results for the OH + HNO₃ → H₂O + NO₃ reaction, the standard enthalpies of formation from the NIST-JANAF Thermochemical Tables for OH (38.99 ± 1.21 kJ mol⁻¹), H₂O (-241.826 ± 0.042 kJ mol⁻¹), NO₃ (71.13 ± 20.9 kJ mol⁻¹) and HNO₃ (-134.31 ± 0.42 kJ mol⁻¹) [40], and the experimental fundamental modes of vibration for NO₃ (1050 a₁', 762.3 a₂'', 1492.4 e' and 360 e' cm⁻¹) [38,41,42], Table S4.

The Potential Energy Surfaces of NO₃ radical reactions can consequently not be described accurately at the theoretical level employed in the present study. In most cases the electronic barrier of a NO₃ radical reaction will occur on a path between the reactant and a *C*_{2v}-like NO₃ radical structure (2*s*1*l*), and the product(s). This part of the PES can be characterised reasonably well. The path connecting the electronic ground state of the NO₃ radical and the *C*_{2v}-like pre-reaction NO₃ radical structure cannot.

The CH₂NN + NO₃ reaction parallels that of the OH radical; the C-addition route is extremely exothermic, without any entrance barrier and leading to formaldehyde. We locate a relatively high barrier to the N-addition reaction (~65 kJ mol⁻¹) making this route of no importance under atmospheric conditions.



The C-addition reaction 15a proceeds in three steps: (1) a barrierless addition of the NO₃ radical to the carbon atom, (2) an almost barrierless elimination of N₂ to give

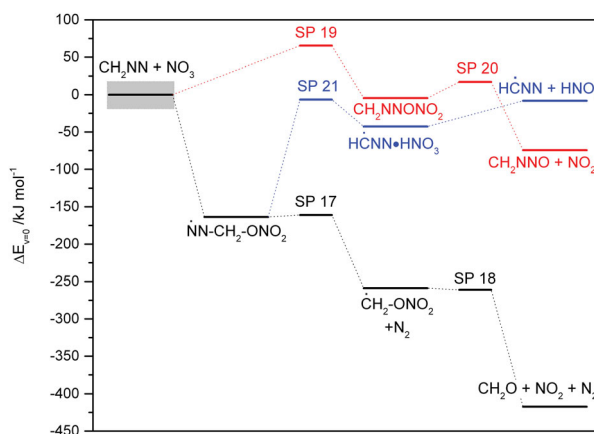
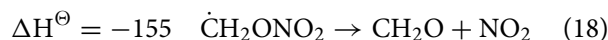
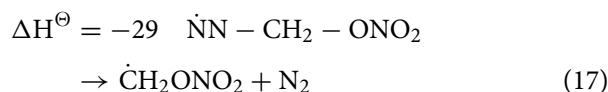
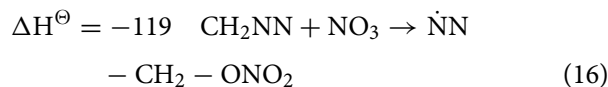
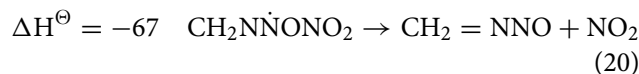
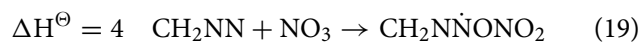


Figure 4. Stationary points on the potential energy surface of the CH₂NN + NO₃ reaction. Results from CCSD(T*)-F12a/aug-cc-pVTZ//M06-2X/aug-cc-pVTZ calculations. The grey box illustrates the inherent uncertainty in the electronic energy of the NO₃ radical.

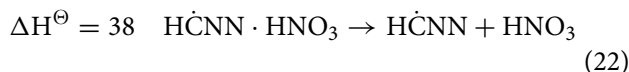
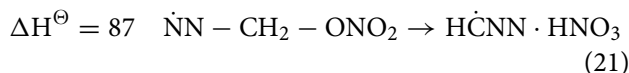
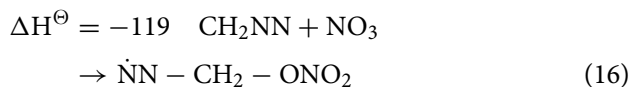
CH₂ONO₂, and (3) an essentially barrierless elimination of NO₂ as illustrated in Figure 4 (the underlying quantum chemistry data are collected in Table S5):



The N-addition reaction 15b proceeds via the CH₂NNONO₂ radical and a second barrier around 40 kJ mol⁻¹ above the entrance energy of reactants to give N-nitroso methanimine:



Finally, the H-abstraction reaction is found to be nearly thermoneutral and to proceed via the $\dot{\text{N}}\text{N}-\text{CH}_2-\text{ONO}_2$ radical on the entrance side and a strong H-bonded complex, HCNN·HNO₃, on the exit side:



Although the barrier to H-abstraction is calculated to fall below the entrance energy of the initial reactants (Figure 4), the competing ejection of N₂ from NN-CH₂-ONO₂ radicals, which has virtually no barrier, will completely dominate the atmospheric fate of the NN-CH₂-ONO₂ adduct.

As mentioned above, the electronic energy of the NO₃ radical is calculated indirectly by aligning the theoretical results for the OH + HNO₃ → H₂O + NO₃ reaction to the standard enthalpies of formation listed in the NIST-JANAF Thermochemical Tables [40]. The experimental enthalpy of formation of the NO₃ radical is associated with a large uncertainty, which transfers into a large uncertainty in the initial energy of the reactants as indicated in Figure 4. The potential energy surface of the CH₂NN + NO₃ reaction is, however, of such a nature that a systematic error of this magnitude has no impact on the theoretically predicted kinetics and dynamics: (1) the reaction will take place with a rate close to the collision limit, and (2) the reaction will proceed entirely via addition to the C-atom resulting in CH₂O as the sole organic product.

Conclusions

Diazomethane, a potential intermediate in the atmospheric degradation of methylamine, is shown to react very fast with OH and NO₃ radicals and relatively fast with O₃, with room temperature rate coefficients of respectively 1.68×10^{-10} , $> 10^{-11}$ (conservative estimate from experiments; $> 10^{-10}$ according to theoretical results) and 3.2×10^{-17} cm³ molecule⁻¹ s⁻¹. On a global scale reaction with OH radicals is the dominant gas phase loss process for a majority of tropospheric trace gases [8]. The OH radicals are mainly produced photolytically, and the OH radical is only present at significant concentrations during the daylight hours. The NO₃ radical photolyses rapidly [43], and NO₃ radical concentrations are low during daylight hours but can become elevated at night. Measured ground-level NO₃ radical concentrations range up to 1×10^{10} cm⁻³, and a 12-hour night-time average concentration of $\approx 5 \times 10^8$ cm⁻³ have been proposed [28,43]. An unpretentious comparison of the atmospheric sinks for diazomethane, based on annual global average oxidant concentrations ([OH]_{24h} = 10^6 cm⁻³, [O₃]_{24h} = 10^{12} cm⁻³ (40 ppbV) and [NO₃]_{12h} = 10^8 cm⁻³), places the atmospheric lifetime of diazomethane to be around 1½ hour with respect to reaction with OH radicals, 8 h with respect to reaction with O₃ and only 15 min with respect to reaction with NO₃ radicals.

In conclusion, diazomethane will have a very short atmospheric lifetime – a few hours during daytime and a

few minutes during night time with formaldehyde being the sole product. Direct photolysis will rarely be important, and atmospheric removal by acidic aerosol hydrolysis will only be important in special situations.

Disclosure statement

No potential conflict of interest was reported by the authors.

Funding

This work is part of the Atmospheric Chemistry of Amines project (ACA) supported by the CLIMIT program under contract 244055 and has received additional support from the Research Council (Norges Forskningsråd) of Norway through its Centres of Excellence scheme, project number 262695.

ORCID

Claus J. Nielsen  <http://orcid.org/0000-0002-2962-2634>

Armin Wisthaler  <http://orcid.org/0000-0001-5050-3018>

References

- [1] G. da Silva, *Environ. Sci. Technol.* **47** (14), 7766 (2013).
- [2] C.R.C. Lindley, J.G. Calvert and J.H. Shaw, *Chem. Phys. Lett.* **67** (1), 57 (1979).
- [3] Y. G. Lazarou, K. G. Kambanis, and P. Papagiannakopoulos, *J. Phys. Chem.* **98** (8), 2110 (1994).
- [4] E.C. Tuazon, W.P.L. Carter, A.M. Winer, and J.N. Pitts, *Environ* **15** (7), 823 (1981).
- [5] R.K. Brinton and D.H. Volman, *J. Chem. Phys.* **19** (11), 1394 (1951).
- [6] J.F. Ogilvie, *Photochem. Photobiol.* **9** (1), 65 (1969).
- [7] F. W. Kirkbride and R. G. W. Norrish, *J. Chem. Soc. (Resumed)* (0), **119** (1933).
- [8] B.J. Finlayson-Pitts and J.N. Pitts, *Atmospheric Chemistry: Fundamentals and Experimental Techniques* (Wiley, New York, 1986).
- [9] D.W. Setser and B.S. Rabinovitch, *Can. J. Chem.* **40** (7), 1425 (1962).
- [10] S. Xu and M.C. Lin, *J. Phys. Chem. A.* **114** (15), 5195 (2010).
- [11] J.F. McGarrity and T. Smyth, *J. Am. Chem. Soc.* **102** (24), 7303 (1980).
- [12] A. Jordan, S. Haidacher, G. Hanel, E. Hartungen, L. Mark, H. Seehauser, R. Schottkowsky, P. Sulzer, and T.D. Mark, *Int* **286** (2-3), 122 (2009).
- [13] F. Arndt, *Org. Synth.* **XV**, 3 (1935).
- [14] F. Arndt, *Org. Synth.* **2**, 461 (1943).
- [15] Y. Zhao and D.G. Truhlar, *Theor. Chem. Acc.* **120**, 215 (2008).
- [16] T.H. Dunning, Jr., *J. Chem. Phys.* **90** (2), 1007 (1989).
- [17] R.A. Kendall, T.H. Dunning, Jr. and R.J. Harrison, *J. Chem. Phys.* **96** (9), 6796 (1992).
- [18] T.B. Adler, G. Knizia and H.-J. Werner, *J. Chem. Phys.* **127** (22), (2007).
- [19] G. Knizia, T.B. Adler and H.-J. Werner, *J. Chem. Phys.* **130** (5), (2009).
- [20] K. Fukui, *Acc. Chem. Res.* **14** (12), 363 (1981).
- [21] L.A. Curtiss, P.C. Redfern and K. Raghavachari, *J. Chem. Phys.* **126**, 084108 (2007).

- [22] H.-J. Werner, P. J. Knowles, G. Knizia, F.R. Manby, M. Schütz, P. Celani, T. Korona, R. Lindh, A. Mitrushenkov, G. Rauhut, K.R. Shamasundar, T.B. Adler, R.D. Amos, A. Bernhardsson, A. Berning, D.L. Cooper, M.J.O. Deegan, A.J. Dobbyn, F. Eckert, E. Goll, C. Hampel, A. Hesselmann, G. Hetzer, T. Hrenar, G. Jansen, C. Köppl, Y. Liu, A.W. Lloyd, R.A. Mata, A.J. May, S.J. McNicholas, W. Meyer, M.E. Mura, A. Nicklass, D.P. O'Neill, P. Palmieri, D. Peng, K. Pflüger, R. Pitzer, M. Reiher, T. Shiozaki, H. Stoll, A.J. Stone, R. Tarroni, T. Thorsteinsson, and M. Wang, MOLPRO, version 2012.1, a package of *ab initio* programs (see <http://www.molpro.net>)
- [23] M.J. Frisch, G.W. Trucks, H.B. Schlegel, G.E. Scuseria, M.A. Robb, J.R. Cheeseman, G. Scalmani, V. Barone, B. Mennucci, G.A. Petersson, H. Nakatsuji, M. Caricato, X. Li, H.P. Hratchian, A.F. Izmaylov, J. Bloino, G. Zheng, J.L. Sonnenberg, M. Hada, M. Ehara, K. Toyota, R. Fukuda, J. Hasegawa, M. Ishida, T. Nakajima, Y. Honda, O. Kitao, H. Nakai, T. Vreven, J.A. Montgomery Jr., J.E. Peralta, F. Ogliaro, M. Bearpark, J.J. Heyd, E. Brothers, K.N. Kudin, V.N. Staroverov, R. Kobayashi, J. Normand, K. Raghavachari, A. Rendell, J.C. Burant, S.S. Iyengar, J. Tomasi, M. Cossi, N. Rega, J.M. Millam, M. Klene, J.E. Knox, J.B. Cross, V. Bakken, C. Adamo, J. Jaramillo, R. Gomperts, R.E. Stratmann, O. Yazyev, A.J. Austin, R. Cammi, C. Pomelli, J.W. Ochterski, R.L. Martin, K. Morokuma, V.G. Zakrzewski, G.A. Voth, P. Salvador, J.J. Dannenberg, S. Dapprich, A.D. Daniels, O. Farkas, J.B. Foresman, J.V. Ortiz, J. Cioslowski, D.J. Fox, Gaussian09, Revision B.01 (Gaussian, Inc., Wallingford CT, 2009).
- [24] D.A. Ramsay, *J. Chem. Phys.* **17**, 666 (1949).
- [25] B.L. Crawford, Jr., W.H. Fletcher and D.A. Ramsay, *J. Chem. Phys.* **19**, 406 (1951).
- [26] C.B. Moore, *J. Chem. Phys.* **39** (7), 1884 (1963).
- [27] R. Atkinson, D.L. Baulch, R.A. Cox, J.N. Crowley, R.F. Hampson, R.G. Hynes, M.E. Jenkin, M.J. Rossi, and J. Troe, *Atmos* **6**, 3625 (2006).
- [28] R. Atkinson, *J. Phys. Chem. Ref. Data.* **20** (3), 459 (1991).
- [29] A. Papakondylis and A. Mavridis, *J. Phys. Chem. A.* **103** (9), 1255 (1999).
- [30] A.P. Cox, L.F. Thomas and J. Sheridan, *Nature.* **181** (4614), 1000 (1958).
- [31] A. Kalemios and A. Mavridis, *J. Chem. Phys.* **129** (5), 054312 (2008).
- [32] V.G. Tyuterev, S. Tashkun, P. Jensen, A. Barbe, and T. Cours, *J* **198** (1), 57 (1999).
- [33] Release 19, April 2018, Editor: Russell D. Johnson III. <http://cccbdb.nist.gov/> DOI:10.18434/T47C7Z ed
- [34] T.J. Lee and P.R. Taylor, *Int. J. Quant. Chem.: Quant. Chem. Symp.* **23**, 200 (1989).
- [35] C.L. Janssen and I.M.B. Nielsen, *Chem. Phys. Lett.* **290**, 423 (1998).
- [36] T.J. Lee, *Chem. Phys. Lett.* **372**, 362 (2003).
- [37] W. Eisfeld and K. Morokuma, *J. Chem. Phys.* **113** (14), 5587 (2000).
- [38] T. Ishiwata, I. Tanaka, K. Kawaguchi, and E. Hirota, *J* **82** (5), 2196 (1985).
- [39] K. Kawaguchi, E. Hirota, T. Ishiwata, and I. Tanaka, *J* **93** (2), 951 (1990).
- [40] M. W. Chase, *NIST-JANAF thermochemical tables* (National Institute of Standards and Technology, Washington, D.C.; Woodbury, N.Y., 1998).
- [41] T. Ishiwata, I. Fujiwara, Y. Naruge, K. Obi, and I. Tanaka, *J* **87** (8), 1349 (1983).
- [42] R.R. Friedl and S.P. Sander, *J. Phys. Chem.* **91** (11), 2721 (1987).
- [43] R.P. Wayne, I. Barnes, P. Biggs, J.P. Burrows, C.E. Canosamas, J. Hjorth, G. Lebras, G.K. Moortgat, D. Perner, G. Poulet, G. Restelli, and H. Sidebottom, *Atmos* **25A** (1), 1 (1991).